VLBI2010 Simulations Using SOLVE

D.S. MacMillan
NVI, Inc. and NASA Goddard Space Flight Center
Greenbelt, Maryland USA 20002

Abstract. To design the future VLBI2010 system, the IVS is performing simulations to determine optimal network antenna locations, antenna sensitivities, slew rates, and observing schedules. I am developing a simulation procedure for testing different observing system parameters using the SOLVE VLBI analysis system. Here I describe the general procedure that is followed, validation and calibration of the simulation procedure, and simulation results for networks of increasing number of antennas.

Keywords. VLBI, simulation, VLBI2010

1 Introduction

The IVS is engaged in the design of a new observing system VLBI2010 (Niell et al., (2005)) that will consist of small (at least 12 m diameter) fast-slewing antennas. The goal is to choose antennas that are mechanically reliable and that can be reproduced economically to allow more international VLBI groups to be able to afford to install antennas. The result would be a superior global coverage with VLBI antennas which currently has poor Southern Hemisphere coverage. The smaller collecting area of the envisioned VLBI2010 antennas will be compensated for with data sampling over 3 or 4 continuous frequency bands from 2 to 15 GHz at a much higher data rate, for example, 8 to 32 Gbps, compared to the current operational rates of 128 or 256 Mbps. As part of the development of specifications for VLBI2010, it is necessary to investigate the geodetic performance of networks of nominal VLBI2010 antennas. To do this, I am developing a Monte Carlo procedure for simulating the performance of a specific observing scenario. In this paper, I describe the procedure, provide some examples of simulation validations where simulation results are compared with results from actual observations, and discuss results of network simulations.

2 Simulation Procedure

The first step in the simulation procedure is to specify the network site locations, antenna sensitivities, antenna slew rates, and observation SNR requirements. We then run the SKED (xxxx) program to generate an observation schedule for a 24-hour VLBI experiment session and a simulation observation file corresponding to the schedule. The next step is to run the VLBI SOLVE (Ma et al. (1990)) analysis program with a simulation data file to estimate parameters (for example, Earth orientation parameters (EOP) and site positions) in the same way as in the analysis of observed data.

To determine the precision (repeatability) of estimated parameters, a Monte Carlo simulation is performed by making repeated VLBI SOLVE runs with the same 24-hour observation file but with different input simulated observed delays. In the current simulation procedure, we generate simulate wet zenith delays and clock delays for each station as random walk processes. It is also possible to add gradient or turbulence (as equivalent wet zenith) delay contributions. Summarizing, the current model for the observed simulation delay is

$$[m_w(\varepsilon_2)\tau_{wz2} + clk_2] - [m_w(\varepsilon_1)\tau_{wz1} + clk_1] + \sigma_{obs} \qquad (1)$$

where m_w is the wet mapping function and ε_1 and ε_2 are the observation angles at sites 1 and 2. The τ_{wz} and *clk* terms are the wet zenith and clock delays at the two sites. To model, observation uncertainty, we add a corresponding white noise contribution, σ_{obs}

3 Simulation Validation

In order to see how simulation results compare with observed results, I have run simulated observations through SOLVE using observing schedules that were used for actual VLBI experiments. We believe that the dominant VLBI errors are a combination of atmospheric and clocklike (maser + instrumental) errors. To simulate these errors, I generated wet zenith delays and clock delays as random walk processes as described above.

3.1 CONT05 Test

In September 2005, the IVS conducted a series of experiment sessions called CONT05 for a period of 15 consecutive days. These sessions were scheduled with nearly the same observing schedule. To test the simulation procedure, I generated simulated observed delays as random walk processes with typical expected atmosphere and clock variances. In previous work, we found that atmospheric variances computed from delay rate residuals using the Kalman filter procedure KALAN (Herring et al., (1990)) are in the range from 0.1 to 0.6 ps^2/s but are usually less than 0.3 ps^2/s (MacMillan, (1992)). Three simulations were run. In the first case, for all sites random walk variances were 0.1 ps^2/s for the wet zenith troposphere and 0.3 ps^2/s for the clock, which corresponds to an Allan standard deviation of 10^{-14} @ 50 minutes. In the second, the random walk variances were 0.3 ps^2/s for the atmosphere and 1.2 ps^2/s for the clock, which corresponds to $2x10^{-14}$ @ 50 minutes. In the third, random walk variances were increased to 0.5 ps^2/s. For each case, 15 ps was added to observation uncertainties and random noise with standard deviation equal to observation uncertainty was added. In our standard processing with SOLVE, this is about the level of noise that is added to observation uncertainties in reweighting of observations to make the solution χ^2 per degree of freedom unity.

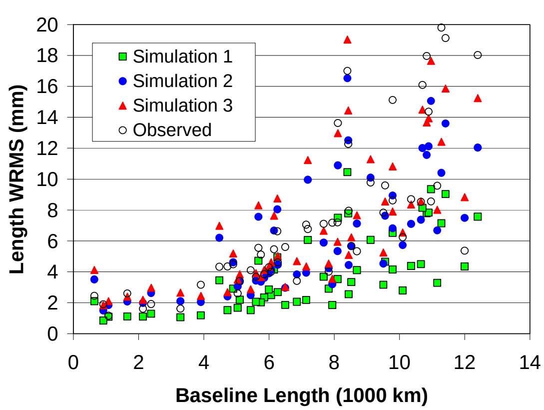

Fig. 1. Comparison of simulated versus observed CONT05 baseline length WRMS. Simulation 1: atmos 0.1 ps^2/s, clock 0.3 ps^2/s; Simulation 2: atmos 0.3 ps^2/s, clock 1.2 ps^2/s, Simulation 3: 0.5 ps^2/s, clock 1.2 ps^2/s.

Figure 1 compares the WRMS (weighted root mean square) baseline length repeatability from simulations with the observed repeatability. The last two simulations yield repeatabilities that are reasonably close to the observed values.

Another test that can be made is to look at the precision of EOP estimates. For this simulation, I computed the repeatability of EOP estimates over the sequence of 15 CONT05 sessions. Table 1 provides a comparison of the simulation EOP precision, the formal EOP uncertainty, and the WRMS difference between VLBI and IGS (International GNSS Service) EOP estimates.

Table 1. Simulation EOP precision for CONT05

Parameter	Simulation Precision	Formal Error	VLBI-IGS WRMS
X (μas)	54	30	55
Y (μas)	69	30	36
UT1 (μs)	3.7	1.3	---
Xr (μas/d)	277	92	198
Yr (μas/d)	178	87	158
LOD (μs/d)	6.4	3	16

In our geodetic analysis with the SOLVE program, we generally find that our parameter formal uncertainties underestimate observed precision by a factor of 1.5 to 2. The simulation precision values tend to be larger than the formal uncertainties by a somewhat larger factor. Except for LOD, the WRMS differences between observed VLBI and IGS EOP during the CONT05 period are comparable to the simulation precision. It is not understood why the simulation precision for Y-pole estimates is somewhat worse than for X-pole; whereas, it is significantly better in the observed data. Network geometry should be reflected in the formal uncertainties, which for CONT05 indicate that the X and Y precision are equal and therefore more consistent with the simulation.

3.2 CORE-NEOS Test

One of the ways that we can measure the accuracy of VLBI EOP estimates is by analyzing the differences between EOP estimated from two independent VLBI networks that observed simultaneously on the same days. From 1997 to 2000, a bi-monthly series of 80 24-hour VLBI experiments, the CORE-A series, were conducted on the same day as a corresponding weekly operational NEOS-A experiment. To see how consistent simulated data is with observed data, we ran a Monte Carlo solution in which simulated data was run through all of the CORE-NEOS session observing schedules. In this case we used random walk variances of 0.5 ps^2/s for the atmosphere and 0.3 ps^2/s for clocks. I estimated EOP for all sessions and computed the RMS difference between simulated EOP from the 80 simultaneous pairs of 24-hour experiments. Table 2 shows the results from the simulation along with differences for observed data. The CORE-NEOS differences are remarkably similar to the observed differences.

Table 2. WRMS differences between EOP determined by the CORE-A and NEOS-A simultaneous experiment sessions

Parameter	Simulation	Observed
X (µas)	191	203
Y (µas)	223	151
UT1 (µs)	9.4	8.6
Psi (µas)	326	367
Eps (µas)	110	142
Xr (µas/d)	462	523
Yr (µas/d)	542	544
LOD (µs/d)	23	19

4 Recovery of Input Noise

The network simulations reported in this paper used simulated input atmospheric delay based on a random walk wet zenith troposphere model.

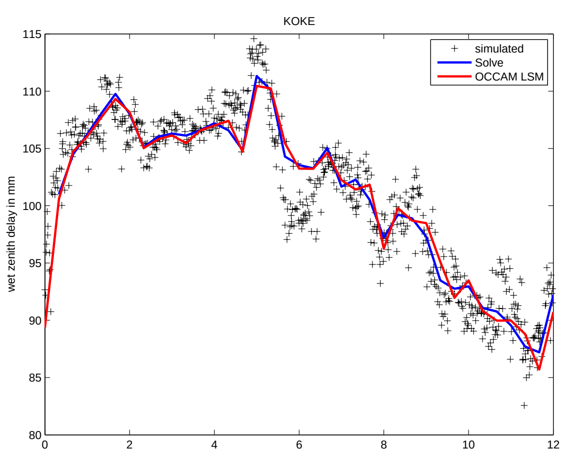

Fig. 2. Comparison of input equivalent wet zenith delay in mm at Kokee Park (Hawaii) (crosses) from a turbulence model with recovered wet zenith delay estimates using the SOLVE (solid blue line) and OCCAM (solid red line) analysis programs. (Figure courtesy of J. Böhm)

One of the issues investigated by the IVS VLBI2010 committee is what is the effect of using turbulent model delays in simulations rather than the simple wet zenith delay random walk. To obtain realistic simulations, we clearly need to use realistic tropospheric delays. T. Nilsson at Chalmers University of Technology (Onsala) generated turbulent delays for given observing schedules assuming Kolomogorov turbulence. Previous work on this was described in Nilsson et al. (2005).

Comparisons in Figure 2 between the input equivalent wet zenith delay input from the turbulence model and the estimated wet zenith delay using SOLVE or OCCAM shows that there are periods of time where recovery of the input model is poor. This implies that the delay from the turbulent model is not well-modeled as the product of an azimuthally symmetric wet mapping function and a wet zenith delay as given by equation (1). On the other hand, if the model input (for example, wet zenith delay random walk) has the same form as the estimation model as in equation (1), we may get unrealistic results that underestimate the atmospheric delay error.

5 Network Simulations

For VLBI2010, we would like to design a global network of antennas to optimize the precision of estimated parameters. Here, I will discuss simulations to determine the dependence of EOP and reference frame scale precision on the number of sites in the network. Simulations were run for the network of 32 sites shown in Figure 3 and then for a sequence of subset networks of 24, 16, and 8 sites. These networks were chosen to provide better global coverage than current VLBI networks and approximately even distribution of sites between the Northern and Southern hemispheres. The antennas used in the simulation were nominal VLBI2010 12-meter antennas with system equivalent flux density (SEFD) of 2500 Jy. The data rate was chosen to be 8 Gbps. For the simulation runs, the wet zenith delays and clock delays were generated with random walk variance of 0.5 ps^2/s and 0.3 ps^2/s.

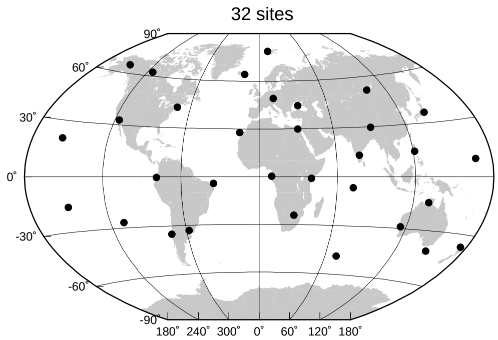

Fig. 3. Global network of 32 sites used for simulations

To estimate the precision of EOP, I ran a solution to estimate EOP in a Monte Carlo run in which the 24-hour simulation observation file was run with different input simulated delays for each of 25 repetitions. The WRMS of the estimated EOPs was taken to be the simulated EOP precision. As a function of network size, Figure 4 shows the EOP precision relative to the 8-station network precision. This relative precision improves by about a factor of two in going from 8 sites to 32 sites, but tends to level off for networks with more than 16 sites.

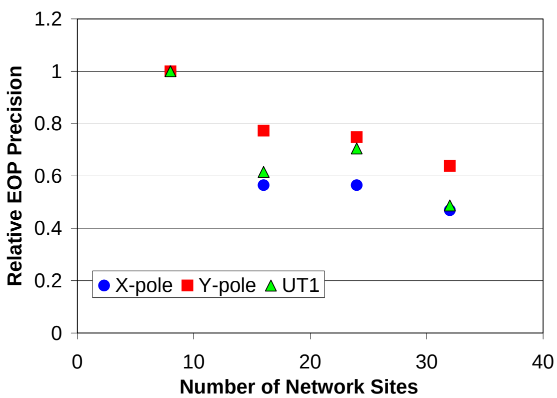

Fig. 4. EOP precision improvement with a larger network size based on Monte-Carlo simulations. Precision is given relative to the 8-site network precision for X-pole (circle), Y-pole (square), and UT1 (triangle).

To obtain an estimate of the terrestrial reference frame scale precision for a given network, I estimated a scale parameter for each of 25 solution repetitions. In this solution, site positions were not estimated so that any residual motion resulting from simulated delays would be propagated only to the estimated network scale parameter. Scale precision from the simulation is the WRMS of the scale

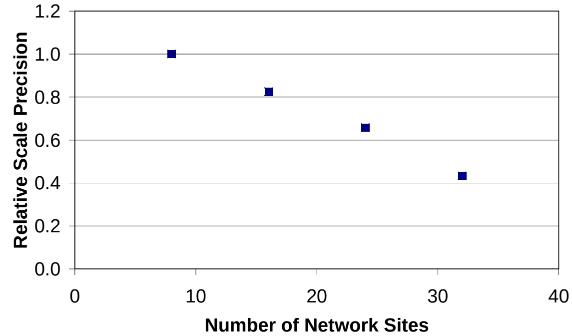

Fig. 5. Reference frame scale parameter precision from Monte-Carlo simulations. Precision is expressed relative to the precision of the 8-site network.

parameter estimates over the series of 25 repetitions. As illustrated in Fig. 5, scale precision improves with network size, where precision is given relative to the 8-site precision. As for EOP, precision improves by about a factor of two with a 32-site network. In contrast, the improvement appears to be nearly linear and does not level off for networks with more than 16 sites.

6 Summary

I have used the Monte Carlo method to determine expected precision of estimated geodetic parameters for global networks of VLBI2010 antennas. Comparisons between statistics of the simulation estimates and estimates from actually observed VLBI sessions show reasonably good agreement. Simulations of global networks of VLBI2010 antennas show that EOP and TRF scale precision improves by about a factor of 2 if the number of network sites increases from the current typical number of 8 sites up to 32 sites. For EOP, most of this improvement occurs in moving up to about 20 sites.

References

Herring, T.A., J.L. Davis, and I.I. Shapiro (1990). Geodesy by Radio Interferometry: The Application of Kalman Filtering to the Analysis of VLBI Data. *Journal of Geophysical Research*, 95(B8), pp. 12561-12582.

Ma, C, J.M. Sauber, L.J. Bell, T.A. Clark, D. Gordon, W.E. Himwich, and J.W. Ryan (1990). Measurement of Horizontal Motions in Alaska Using Very Long Baseline Interferometry. *Journal of Geophysical Research*, 95(B13), pp. 21991-22011.

MacMillan, D.S. and J.R. Ray (1991). Current Precision of VLBI Vertical Determinations. In: *Proceedings of the AGU Chapman Conference on Geodetic VLBI: Monitoring Global Change*, pp. 428-436.

Niell, A., A. Whitney, B. Petrachenko, W. Schlüter, N. Vandenberg, H. Hase, Y. Koyama, C. Ma, H. Schuh, and G. Tucari (2005). VLBI2010: Current and Future Requirements for Geodetic VLBI Systems, Report of Working Group 3 to the IVS Directing Board.

Nilsson, T. and L. Gradinarsky, and G. Elgered (2005). Correlations Between Slant Wet Path Delays Measured by Microwave Radiometry. *IEEE Transactions on Geoscience and Remote Sensing*, 43(5), pp. 1028-1035.